24th COBEM - 2017

24th ABCM International Congress of Mechanical Engineering
December 3-8, 2017, Curitiba, PR, Brazil

COBEM-2017-1199
FREE-SURFACE MODELING EMPLOYING A TWO-WAY FLUID-STRUCTURE INTERACTION APPROACH FOR THE FLOW AROUND A CIRCULAR CYLINDER

Fernando Mattavo de Almeida
Gustavo Roque da Silva Assi
Universidade de São Paulo – Escola Politécnica - Naval Architecture and Oceanic Engineering Department
fernando.mattavo.almeida@usp.br ; g.assi@usp.br

Abstract. *For some oceanic engineering applications such as tidal power generation and other flow patterns that involves open channels, the correct approach for free surface modelling is mandatory. The deformation of free surface is responsible for increasing confinement and enhance the turbine power extracted and efficiency. The classical approach for oceanic waves used potential flow theory with constant pressure and no normal velocity through free surface. This model includes to buoyancy effects in energy conservation. Although, can be analytically proven that inducing surface pressure in interface between water and air with the same value of static pressure on the seabed and neglecting buoyancy effects, the resulting differential equations are the same at both models. The same conclusion can be found in the Navier-Stokes equation at the free surface. The main difference between the two approaches is the vertical thrust that appears due to vertical pressure gradient produced by body force effects. However, this force is easily calculated analytically.*
This approach could be modelled as an elastic wall over the surface. this elastic wall could be simulated by a solid body with orthotropic mechanical properties. The body must be modelled in order to heave stiffness only in gravity direction and has no shear resistance. Therefore, for solving this problem, is needed the coupling between static structural model and fluid model. Considering that the deformation of free surface is responsible for modifying the flow on every iterating, the fluid domain must be recalculated which leads to a new pressure field in the surface. Thus, a 2-way Fluid structure interaction model is required.

Keywords: *Oceanic Engineering, Fluid Structure Interaction, Computational Fluid Dynamics, Free Surface Modelling*

1. INTRODUCTION

Flows subjected to free surfaces appears in different areas. For example, in oil and gas industry with offshore operations, transport vessels and other applications have the influence of the interface between water and air on their flow patterns. Some towing tank experiments have a free surface that have a considerable interference on the results. However, the main motivation of the present paper is focused on oceanic energy exploitation. The ocean has a potential to generate about 2950 TW.h on each year (World Energy Council, 2016). Besides of that, most of this energy could be extracted from surface waves and from tides. Both phenomena have a high influence from the free surface.

Most of analytical models (Houlsby, Draper, & Oldfield, 2007) and (Whelan, Thomson, Graham, & Peiró, 2007) that includes the constant pressure boundary from the free surface assumes this condition as a flow restriction and gives a blockage factor that relates the submerged body cross sectional area to channel cross sectional area. However, for a CFD simulation, is important to determine the free surface shape. The most used method for modelling this phenome is considers a biphasic simulation using an averaged method between the fluid properties known as Volume of Fluid (VOF) Method, however, it is computationally expensive and is accuracy is very dependent from the mesh refinement on the free surface region.

For solving this issue, is proposed an alternative model for free surfaces, considering a monophasic flow confined by an elastic wall. With such model, the confinement effects are accounted and there is no need of buoyancy modelling, thus a steady state calculation is allowed. This elastic wall modelling demands a perfectly elastic body and for accounting this non-linear problem, a two-way fluid structure interaction method is needed. In this paper, both analytical approach is used to calculate the elastic wall properties, which is based on an orthotropic elastic body, analyzing its behavior in steady state and transient state approach and computational methods comparing the accuracy from VOF and this proposed model.

1.1 Model

The main analysis consists in a 2-D flow around a circular cylinder, as shown in Figure 1 in which both fluid depth and cylinder diameter have the same order. The flow velocity is adjusted to reproduce experimental conditions traditionally used for tidal current turbines (Bahaj, W.M.J., & McCann, 2007).

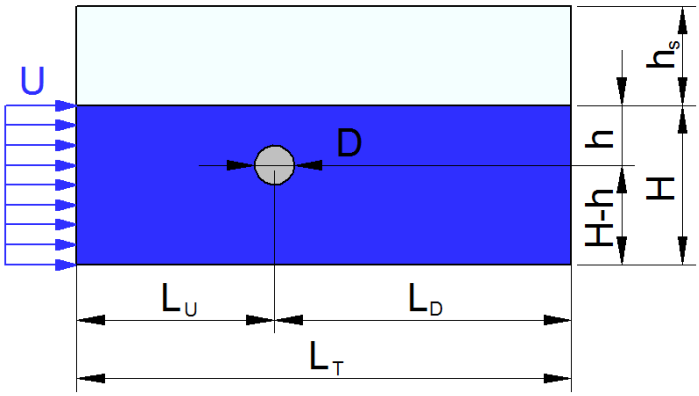

Figure 1 - Schematic drawing of the problem used to compare the different free surface models

The analyzed dimensions are: Domain Length: 20000 mm, Water Depth: 500 mm; Cylinder Depth: 350 mm; Solid/ Air Height: 3000 mm; Upstream Length: 5000 mm; Cylinder Diameter: 100 mm. The velocity of the flow is calculated between 0.5 m/s and 2 m/s which represents a Froude Number from 0.225 to 0.9 and a Reynolds Number between 4,5 x 10^4 and 1.8 x 10^5.

1.2 List of Symbols

The symbols used are shown in Table 1

Table 1 – List of Symbols

Symbol	Definition	Dim.	Symbol	Definition	Dim.
U	Upstream velocity	$L.T^{-1}$	δ_{ij}	Kronecker Delta	$M^0.L^0\ T^0$
L_U	Upstream length	L	μ	Dynamic viscosity	$M.L^{-1}\ T^{-1}$
L_D	Downstream length	L	$F_{i,visc}$	Component "i" of a viscous force	$M.L\ T^{-2}$
L_T	Total domain length	L	α, β, τ	Velocity Coefficient	$M^0.L^0\ T^0$
D	Cylinder diameter	L	ΔH	Height difference	L
H, h_f	Water domain depth	L	$\dot{m}$	Mass flow	$M.L^3\ T^{-1}$
h	Cylinder depth	L	Φ_W	Wave velocity potential function	$L^2\ T^{-1}$
h_s	Air Domain / Solid Domain height	L	V	Potential energy	$M.L^2\ T^{-1}$
t	Time	T	ϕ	Airy's stress function	$M.L^1\ T^{-2}$
u_i, u_j	Velocity vector	$L.T^{-1}$	E	Elasticity Modulus	$M.L^{-1}\ T^{-2}$
x_i, x_j	Coordinate	L	G	Shear Modulus	$M.L^{-1}\ T^{-2}$
ρ	General density	$M.L^{-3}$	ν_{ij}	Poisson Coefficient	$M^0.L^0\ T^0$
p	Pressure	$M.L^{-1}\ T^{-2}$	$\mathcal{T}$	Kinetic energy by unit of length	$M.L\ T^{-1}$
ν	Kinematic viscosity	$L^2\ T^{-1}$	$\mathcal{U}$	Potential energy by unit of length	$M.L\ T^{-1}$
g_i	Gravity Vector	$L\ T^{-2}$	$\mathcal{W}_{nc}$	Non-conservative work	$M.L\ T^{-1}$
p_{hfs}	Pressure due to free surface level	$M.L^{-1}\ T^{-2}$	w_0	Free surface deformation	L
p_{hr}	Harmonic residual pressure	$M.L^{-1}\ T^{-2}$	K_n	Mode "n" constant	$M^0.L^0\ T^0$
p^*	Velocity gradient pressure	$M.L^{-1}\ T^{-2}$	k_m	Wave number	L^{-1}
η	Free surface elevation	L	Ω_m, ω_n	Frequencies	T^{-1}
g	Gravity modulus	$L\ T^{-2}$	ρ_f	Fluid density	$M.L^{-3}$
τ_{ij}	Stress Tensor	$M.L^{-1}\ T^{-2}$	ρ_s	Solid density	$M.L^{-3}$

2. THEORETICAL BASIS

This section is destined to derive the properties from the elastic body that produces the restoring force in substitution from gravity in the standard free surface model. Is proven, for potential flow theory, in which gravity waves are based, that in both steady and transient flow, the alternative model produces exactly the same results from the traditional model. A brief revision from gravity surface waves is made, since this effect governs the free surface deformation in the ocean and some parameters such as wave energy and dispersion relation are needed.

2.1 Comparison between the two free surface models in fluid flow equations

Unsteady Viscous Fluid Flow Approach

The analyzed flow consists in an incompressible viscous flow. The unsteady momentum conservation equation for a Newtonian fluid subjected to an incompressible flow is written below (White F. , Viscous Fluid Flow 3rd Ed., 2006).

$$\frac{\partial}{\partial t}(u_i) + \frac{\partial}{\partial x_j}(u_i u_j) = -\frac{1}{\rho}.\frac{\partial p}{\partial x_i} + \frac{\partial}{\partial x_j}\left[\nu \frac{\partial}{\partial x_j}(u_i)\right] + g_i \quad (1)$$

Deriving this equation in function of x_i and evoking the continuity equation for incompressible fluids, is deduced the Poisson's equation for pressure (Pope, 2000). This equation is fundamental to understand the dynamics of the pressure field and makes possible to decompose the pressure in a harmonic solution (which is solution of Laplace's equation) and the particular solution, related to the velocity gradient components.

$$\frac{\partial^2 p}{\partial x_i^2} = -\rho \frac{\partial u_i}{\partial x_j}.\frac{\partial u_j}{\partial x_i} \quad (2)$$

Dividing the pressure field in three components, the first two components, both solution of the Laplace's equation, the first one related to the free-surface elevation, p_{hfs}, and the other the residual harmonic solution, p_{hr}, and the third component, related to the velocity gradient, p^*, is given:

$$p(x,z,t) = p_{hfs}[\eta(x,t),z] + p_{hr}(x,z,t) + p^*(x,z,t) = \rho.g.[\eta(x,t) - z] + p_{hr}(x,z,t) + p^*(x,z,t) \quad (3)$$

Expanding the Navier-Stokes equation (1) and substituting the decomposed pressure (3), is given respectively for flow direction x and perpendicular to the flow direction z the momentum conservation equations:

$$\frac{\partial}{\partial t}u + \frac{\partial}{\partial x}(u.u) + \frac{\partial}{\partial z}(u.w) = -g\frac{\partial \eta}{\partial x} - \frac{1}{\rho}\frac{\partial p^*}{\partial x} + \nu\frac{\partial^2 u}{\partial x^2} + \nu\frac{\partial^2 u}{\partial z^2} \quad (4)$$

$$\frac{\partial}{\partial t}w + \frac{\partial}{\partial x}(u.w) + \frac{\partial}{\partial z}(w.w) = -g\frac{\partial \eta}{\partial z} - \frac{1}{\rho}\frac{\partial p^*}{\partial z} + \nu\frac{\partial^2 w}{\partial x^2} + \nu\frac{\partial^2 w}{\partial z^2} \quad (5)$$

There are two conditions for free surface, the first one states that the pressure is equal the surface tension in free surface and the other that the pressure material derivative is zero in free surface (Newman, 1977). However, for open channel flows, the effects of surface tension could be neglected (White, Conditions at a Free Liquid Surface, 2006). The two conditions are mathematically given by:

$$p(x, z=\eta, t) = 0 \; ; \; \frac{D}{Dt}(p)\Big|_{z=\eta} = 0 \rightarrow \left(\frac{\partial p}{\partial t} + u.\frac{\partial p}{\partial x} + w.\frac{\partial p}{\partial z}\right)\Big|_{z=\eta} = 0 \quad (6)$$

The pressure condition in free surface leads to the pressure fluctuation term in equations (4) and (5) vanishes at free surface. Then, the Navier-Stokes equation written at free surface becomes:

$$\frac{\partial}{\partial t}(u_i) + \frac{\partial}{\partial x_j}(u_i u_j) = -g.\frac{\partial \eta}{\partial x_i} + \frac{\partial}{\partial x_j}\left[\nu \frac{\partial}{\partial x_j}(u_i)\right] \quad (7)$$

This equation shows that flow dynamics is not dependent from gravity vector direction, only from free surface dynamics. The right hand of Navier-Stokes equation is known as gradient from a stress tensor. Since the first term of the right hand is directly proportional to the free surface elevation gradient, can be concluded that the stress tensor is directly dependent from free surface elevation.

The same equation is achieved neglecting the gravity and assuming that on the free surface, pressure is given by:

$$p_{FS}(x, z = \eta, t) = \rho . g . \eta(x, t) + \rho . g . h_f \quad \textbf{(8)}$$

However, the main goal of this work is to analyze the forces acting on the submerged cylinder. For any object subjected to a surface stress tensor such as a cylinder in a fluid flow, the surface force is given by the surface integral of the stress tensor in its boundary. However, the Gauss Theorem could be used to transform the surface integral into a volume integral, as shown in the following equation:

$$\vec{F} = \iint_{S_B} \tau_{ij} n_i . d\mathcal{S} = \iiint_{\mathcal{V}_B} \frac{\partial \tau_{ij}}{\partial x_i} . d\mathcal{V} \quad \textbf{(9)}$$

For a Newtonian fluid approach, the stress tensor is dived in a diagonal matrix, proportional to pressure and in a symmetric matrix related to the fluid velocity gradient, composing the shear stresses (White(b), 2006). Substituting this definition in equation (9) the force is decomposed in a viscous component and in a pressure component:

$$\vec{F} = \iiint_{\mathcal{V}_B} \frac{\partial}{\partial x_i}\left[-p\delta_{ij} + \mu\left(\frac{\partial u_i}{\partial x_j} + \frac{\partial u_j}{\partial x_i}\right)\right] . d\mathcal{V} = \iiint_{\mathcal{V}_B} -\frac{\partial p}{\partial x_i} + \frac{\partial}{\partial x_j}\left(\mu \frac{\partial u_i}{\partial x_j}\right) . d\mathcal{V} = -\iiint_{\mathcal{V}_B} \frac{\partial p}{\partial x_i} . d\mathcal{V} + F_{i,visc} \quad \textbf{(10)}$$

The difference between the buoyancy based model and the free surface modelled as an elastic support is related to the hydrostatic pressure, that enters in the force in the volume integral from pressure gradient. Comparing the results from both models, first for traditional model and then for the proposed model:

$$\vec{F}_p = -\boldsymbol{e_x} \iiint_{\mathcal{V}_B} \left(\frac{\partial p^*}{\partial x} + \rho . g . \frac{\partial \eta}{\partial x}\right) d\mathcal{V} - \boldsymbol{e_z}\left[\iiint_{\mathcal{V}_B} \left(\rho . g . \frac{\partial \eta}{\partial z} + \frac{\partial p^*}{\partial z}\right) d\mathcal{V} + \rho . g . \mathcal{V}_B\right] \quad \textbf{(11)}$$

$$\vec{F}_p = -\boldsymbol{e_x} \iiint_{\mathcal{V}_B} \left(\frac{\partial p^*}{\partial x} + \rho . g . \frac{\partial \eta}{\partial x}\right) d\mathcal{V} - \boldsymbol{e_z} \iiint_{\mathcal{V}_B} \left(\rho . g . \frac{\partial \eta}{\partial z} + \frac{\partial p^*}{\partial z}\right) d\mathcal{V} \quad \textbf{(12)}$$

Is seen, by comparison between (11) and (12) that only significant difference between the models is the buoyancy force, which could be analytically calculated for any submerged body.

Steady State Control Volume Modelling

In order to compare the global effects due to both models, a control volume approach is useful, since only mean values are considered. The model compares the boundary condition with elastic free surface with the traditional actuator disk theory approach with free surface considerations (Whelan, Thomson, Graham, & Peiró, 2007). Other models as open flow and fully confined flow can be found in (Houlsby, Draper, & Oldfield, 2007).

The base domain and analyzed sections are shown in Figure 2. This model is based on the energy conservation by Bernoulli's Equation, mass conservation and momentum conservation equation for one dimensional mean flow (White F. M., 1998). Assuming for both models the same head difference, applying the continuity equation on by-pass region and in streamtube region, are deduced the factor β :

$$\beta = \frac{[H_U(\tau - 1) - \tau \Delta H]\alpha}{(\tau - \alpha)F} \quad \textbf{(13)}$$

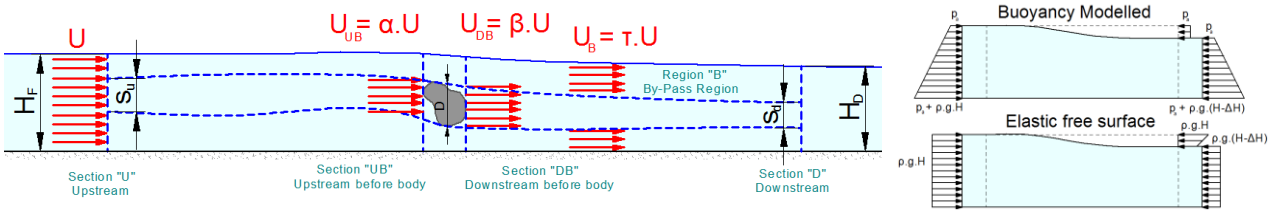

Figure 2 - Control Volume Model for Drag Calculation (Left) and pressure distribution for both models (right)

Table 2 - Differences between elastic free surface and standard model for control volume approach

Parameter	Buoyancy Model	Elastic Free Surface Model
Pressure on free surface	$p_{FS} = p_a$	$p_{FS} = \rho.g.(\eta + H_F)$
Depth difference between upstream and downstream sections	$\Delta H = \frac{U^2}{2g}(\tau^2 - 1)$	$\Delta H = \frac{U^2}{2g}(\tau^2 - 1)$
Force actuating on the body	$F = \frac{\rho g}{2}[2.H_U.\Delta H - (\Delta H)^2] + \sum \dot{m}V$	$F = \frac{\rho g}{2}[2.H_U.\Delta H - (\Delta H)^2] + \sum \dot{m}V$

From Bernoulli equation, calculated through a streamline on the free surface, for traditional and proposed model, respectively, is calculated the same height difference. This result is shown in the equations (14) and (15) below:

$$\rho.g.H_U + \rho\frac{U^2}{2} + p_a = \rho.g.(H_U - \Delta H) + \rho\frac{\tau^2 U^2}{2} + p_a \rightarrow \Delta H = \frac{U^2}{2g}(\tau^2 - 1) \quad \textbf{(14)}$$

$$\rho\frac{U^2}{2} + \rho.g.(H_F) = \rho\frac{\tau^2 U^2}{2} + \rho.g.(-\Delta H + H_F) \rightarrow \Delta H = \frac{U^2}{2g}(\tau^2 - 1) \quad \textbf{(15)}$$

Finally, from momentum conservation, using the pressure distribution shown in Figure 2 is given, for the traditional model and for the proposed model, respectively:

$$\sum F_{ext} + \frac{(2.p_a + \rho.g.H_U)H_U}{2} - p_a\Delta H - \frac{[2.p_a + \rho.g.(H_U - \Delta H)](H_U - \Delta H)}{2} = \sum \dot{m}V \quad \textbf{(16)}$$

$$\sum F_{ext} + \rho.g.H_U^2 - \frac{[\rho.g.H_U + \rho.g.(H_U - \Delta H)]\Delta H}{2} - \rho.g.(H_U - \Delta H)^2 = \sum \dot{m}V \quad \textbf{(17)}$$

The results are summarized in the Table 2, in which is shown that both models produce the same results.

Unsteady Gravity waves modelling by potential flow theory

Considering negligible the turbulent motion and viscosity for surface waves due to involved length scales, is possible to use the potential theory for analyze gravity waves. Calling Φ_W the velocity potential, are analysed the equations derived from the traditional buoyancy based model and the new proposed model with an elastic free surface. The potential function is a harmonic function and is solution from the Laplace Equation (Pope A. , 1951).

Being $\eta = \eta(x,t)$ any aleatory function that describes the free surface elevation. There is no net flux across this boundary. That means that the velocity field normal to the free surface curve is the same as the velocity of the free surface. The other boundary condition considered at free surface is the conservation of energy, as used on the previous section. Was proven that both models lead to the same result from Bernoulli's Equation on the Free Surface. Since the alternative model proposes an elastic wall without shear, the velocity tangential to the free surface is allowed, hence the normal velocity must be the same as the wall. It produces the same boundary conditions for both models. Since the basic equation, the Laplace's Equation, is the same for both models, the result is the same. Therefore, the proposed model is sufficient to calculate gravity waves. The non-linear equation for the free-surface is given below:

$$\frac{1}{g}\frac{\partial^2\Phi_W}{\partial t^2} = -\frac{\partial\Phi_W}{\partial z} - \nabla\Phi_W.\nabla\left[\eta - \frac{1}{g}\frac{\partial\Phi_W}{\partial t}\right] \quad \textbf{(18)}$$

From a linear approach, the last term from hand side on the equation above is neglected. Is deduced the velocity potential for a finite depth assuming no normal velocity on the flow bottom (Newman(b) & J.N., 1977). The dispersion relation, which relates wave length and its frequency is given by:

$$\omega^2 = g.k.tanh(k.h_f) \quad \textbf{(19)}$$

The total energy density is calculated assuming the gravity potential energy from free surface and from velocity field derived from velocity potential. Assuming that the total energy must remain constant, the kinetic energy by unit of surface is given by:

$$\mathcal{T}_W = \frac{1}{2}\rho g(A^2\text{-}\eta^2) \quad \textbf{(20)}$$

2.2 Solid Material properties for free surface elastic body modelling

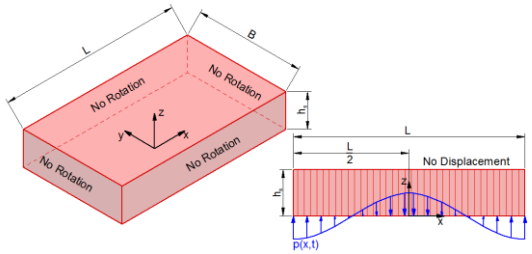

Figure 3 - Orthotropic solid for elastic surface modelling

In order to model correctly the elastic surface, a pressure applied on a point $x = x_0$ must only produces deformations only in the point $x = x_0$ letting all points in the boundary with zero displacement. For modelling such behavior, is necessary to resort to orthotropic materials, since any isotropic elastic solid have a shear modulus that is responsible for accommodate the deformation in all directions. Any continuous media must satisfy the dynamic equilibrium equation, given bellow (Capaldi, 2012):

$$\rho \frac{\partial u_i}{\partial t} + \rho u_j \frac{\partial u_i}{\partial x_j} = \rho g_i + \frac{\partial \tau_{ij}}{\partial x_j} \quad \textbf{(21)}$$

Since the first approach is the steady state calculation, the velocity components of the previous equation are equal to zero. Also considering that all body forces are produced from a conservative field, such as gravity, the body force term could be substituted by the gradient of a potential function. Then, in a bi-dimensional stress field, the equilibrium equation becomes:

$$\frac{\partial^2 \sigma_i}{\partial x_i^2} + \frac{\partial^2 \tau_{ij}}{\partial x_i \partial x_j} = \frac{\partial^2 V}{\partial x_i^2} \quad \textbf{(22)}$$

Calling the Airy's function from traditional isotropic elasticity model and using the relation of compatibility between strain components (Timoshenko & Goodier, 2010), using generalized Hooke's law for orthotropic materials, (Lekhnitskii, 1981) and neglecting the effects of body forces, is deduced the equation of compatibility for orthotropic materials with plane state of strain

$$\frac{\left(1 - \nu_{yz}^2\right)}{E_z} \frac{\partial^4 \phi}{\partial x^4} + \left[\frac{1}{G_{xz}} - \left(\nu_{xz} + \nu_{xy}.\nu_{yz}\right)\left(\frac{1}{E_x} + \frac{1}{E_z}\right)\right] \frac{\partial^4 \phi}{\partial x^2 \partial z^2} + \frac{\left(1 - \nu_{xy}^2\right)}{E_x} \frac{\partial^4 \phi}{\partial z^4} = 0 \quad \textbf{(23)}$$

By hypothesis, all mechanical properties have the same value in all directions and shear modulus is negligible if compared with elasticity modulus. The model used for calculation is shown in Figure 3, where is defined zero displacement in all directions for the solid upper surface, no rotation in all vertical faces and pressure applied on the lower surface. Therefore, the compatibility equation becomes:

$$\frac{1}{G_{xz}} . \frac{\partial^4 \phi}{\partial x^2 \partial z^2} = 0 \quad \textbf{(24)}$$

Considering a pressure field decomposed by a sin-series and assuming that a sin series is solution from (24), the shear stress becomes zero for any load distribution. Comparing the pressure distribution with the normal stress in the pressure direction is deduced that:

$$\delta_z(x) = \int_0^{h_s} \varepsilon_z(x,z).dz = \frac{\left(1 - \nu_{yz}^2\right) h_s}{E_z} \sum_{n=0}^{+\infty} A_n . sin\left(\frac{n\pi x}{L}\right) = k_z p(x) \quad \textbf{(25)}$$

Since the pressure derivative in relation to free surface elevation is equal to $\rho_f . g$, which is the spring constant, is calculated the necessary solid Elasticity model to produces the same results for the model with buoyancy. For simplicity, is assumed that the elasticity model is the same for all directions and the shear modulus and Poisson coefficient are sufficiently small in order to have no influence in the spring constant. The calculated properties are shown in Table 3.

Table 3 - Orthotropic solid mechanical properties

Property	Symbol	Formula
Elasticity Modulus	$E_x = E_y = E_z = E$	$E = \rho.g.h_s$
Shear Modulus	$G_{xy} = G_{xz} = G_{yz} = G$	$G = E \times 10^{-3}$
Poisson Coefficient	$\nu_{xy} = \nu_{xz} = \nu_{yz} = \upsilon$	$\upsilon = 10^{-2}$
Solid Pre-Stress	p_a	$p_a = \rho.g.H_f$

2.3 Transient Potential Flow Coupled with Elastic Solid

For the coupling between solid and fluid is necessary to calculate the inertial properties from the solid. However, considering that even for biphasic flow, the dynamics are governed by water flow, the solid must not resonates and reflects the free surface waves. For the analysis is used the extended Hamilton principle, which states the total energy of the system added from the non-conservative works, integrated along the time is a stationary function (Lanczos, 1949).

$$\delta \int_{t_1}^{t_2} (\mathcal{T} - \mathcal{U} + \mathcal{W}_{nc}).dt = 0 \quad \textbf{(26)}$$

Considering a potential fluid flow and a closed system formed by the solid and fluid, there is no external non-conservative work. Besides of that, the fluid is considered incompressible and no gravity effects are taken in account. Therefore, the potential energy occurs only due to solid strain. The kinetic energy is due to solid motion and fluid particles motion, according to the equation (20). Substituting this on equation (26):

$$\delta \int_{t_1}^{t_2} \int_{0}^{L} \left\{ \frac{1}{2}\rho.g.(A^2 - w_0^2) + \int_0^{h_s} \left[\frac{1}{2}\rho_s \left(\frac{\partial w}{\partial t}\right)^2 + \frac{1}{2}E\left(\frac{\partial w}{\partial z}\right)^2 \right].dz \right\}.dx.dt = 0 \quad \textbf{(27)}$$

Applying the chain rule in the variational and with some algebra, is derived the final equation in the integral form:

$$\int_{t_1}^{t_2} \int_{0}^{L} \left[\left(\rho.g.w_0 - E.\frac{\partial w}{\partial z}\Big|_{z=h_s} \right) \delta w_0 + \int_0^{h_s} \left(\rho_s \frac{\partial^2 w}{\partial t^2} - E.\frac{\partial^2 w}{\partial z^2} \right) \delta w.dz \right].dx.dt = 0 \quad \textbf{(28)}$$

Considering that this integral must be zero for every virtual displacement δw and δw_0, the integrand must be zero in every point of the domain. Mathematically, is deduced the following differential equation with its boundary condition:

$$\frac{\rho_s}{E}\frac{\partial^2 w}{\partial t^2} + \frac{\partial^2 w}{\partial z^2} = 0 \quad \textbf{(29)}$$

$$\rho.g.w_0 - E.\frac{\partial w}{\partial z}\Big|_{z=h_s} \quad \textbf{(30)}$$

The partial differential equation is known as wave equation and is classified as elliptic. Therefore, its solution allows the separation of variables, in which the eigen solution is the product between two separated solutions, one for time and other for the spatial coordinate. The general solution is written by:

$$w_n(x,z,t) = \left[A_n^z.cos\left(K_n \frac{z}{h_s}\right) + B_n^z.sin\left(K_n \frac{z}{h_s}\right) \right].\left\{ A_n^t.cos\left[\frac{K_n.t}{h_s}\sqrt{\frac{E}{\rho_s}} + \varphi_n(x) \right] \right\} \quad \textbf{(31)}$$

The condition of fixed boundary on the solid cancels the term A_n^z. Assuming that the solid face with interface with fluid must be solidary to the fluid free surface movement and the boundary condition from (30) must be satisfied, from a sinusoidal free surface with frequency Ω_m, wave number k_m and amplitude B_m, the displacement becomes:

$$w_n(x,z,t) = B_m.sin\left(\Omega_m.z.\sqrt{\frac{\rho_s}{E}}\right).[cos(\Omega_m.t - k_m x)] \quad \textbf{(32)}$$

The boundary condition (30) states that this solution is valid if:

$$\Omega_m . h_s . \sqrt{\frac{\rho_s}{E}} = tg\left(\Omega_m . h_s . \sqrt{\frac{\rho_s}{E}}\right) \quad \textbf{(33)}$$

The tangent is close to the argument value for small angles, usually lower than 10°. According to (Rao, 2016), the first natural mode of the structure, approached by a rod with free end since the shear could be neglected, is given by:

$$\omega_n = \frac{(2n-1)\pi}{2} \frac{1}{h_s} \sqrt{\frac{E}{\rho_s}};\ \omega_1 = \frac{\pi}{2.\ h_s} \sqrt{\frac{E}{\rho_s}} \quad \textbf{(34)}$$

Therefore, the approach is valid if the exciting frequency is lower than 20% of the first natural frequency from the structure. According to (Meirovitch, 2001), the final response is given by superposing the excitation of each natural mode, which are orthogonal, proven by the expansion theorem. Mathematically, the condition of validity of the hypothesis is given by the equation above, in which is shown that adjusting the density is possible to validate the approach, since maximum exciting frequency is function from mesh size according to dispersion relation for waves.

$$\Omega_{MAX} \leq \frac{\pi}{10.\ h_s . \sqrt{\frac{E}{\rho_s}}} \quad \textbf{(35)}$$

3. COMPUTATIONAL METHODS

The computational methods include a biphasic simulation based on VOF and a coupled fluid-structure method in which pressure is exported from the fluid domain to elastic domain and its deformation is returned to the fluid domain, to recalculated the fluid. For both analysis, the $k-\omega-SST$ method is used for turbulence modelling (Menter, 1992), and for the structural calculation, the finite element method is used. Further information can be found on (ANSYS Inc., 2016) and (ANSYS(b), 2016).

3.1 Steady State Biphasic Simulation

The biphasic flow is simulated through Volume of Fluid (VOF) method, in which the proportion between the two fluid is calculated in each finite volume and then the flow properties are averaged (Ketabdari, 2016). It is computationally expensive in despite of being the most popular method to calculate biphasic immiscible flow. The boundary conditions, shown in Figure 4 are constant velocity on water inlet, opening on water outlet, with zero pressure and water proportion as 1, opening on the upper surface, no-slip wall in the inferior boundary and in cylinder and no fluid proportion defined in the mixed outlet, in the expected free surface region.

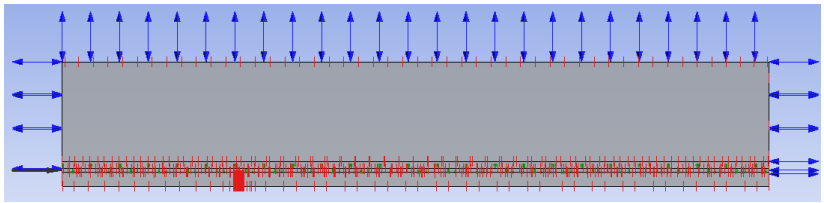

Figure 4 - Boundary Conditions for Biphasic Simulation

3.2 Steady state free surface modelling employing a two-way fluid structure interaction

The boundary conditions for fluid-structure model are shown in Figure 5. The properties from solid model are calculated according to Table 3. The properties are: E = 29,3 kPa, G = 0,03 kPa and υ =0,01. The fluid domain is deformable and the upper face has interface with the solid domain. The solid domain has the same boundary conditions as the analytical model, shown in Figure 3.

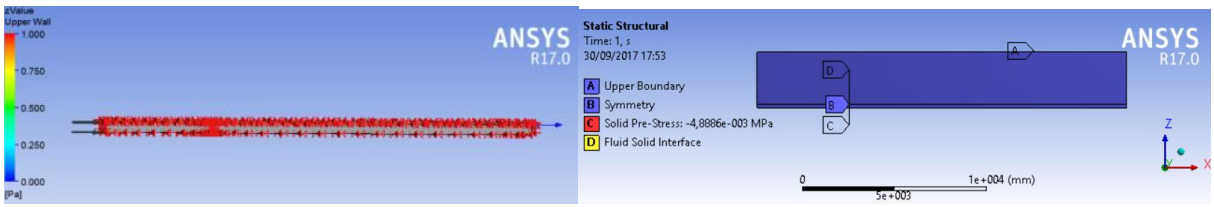

Figure 5 - Fluid-Structure Interaction Boundary Conditions

3.3 Results

From Figure 8 and Figure 9 are shown the experimental data for drag coefficient in a cylinder and the effects of blockage on drag coefficient and vortex shedding frequency. It is used to compare the results obtained from computational methods. The comparison between the free surface shape with the deformation of the solid in the fluid-structure interaction showed some differences and for higher Froude numbers, this effect is increased. However, the total difference of height is almost the same in all tested cases.

The computational time was significantly different between the two models. The biphasic simulation took more time and the needed mesh was higher in order to discretize the free surface correctly. The Fluid-Structure Interaction model required refinement only near to the cylinder while the biphasic model required a reasonable refinement on the free surface mesh, which could cause prohibitive computational costs for complex three-dimensional simulations.

The confinement produced by the free-surface model with an elastic wall was significantly higher near to cylinder and overpredicted the drag in comparison with theoretical results from cylinders in an infinite domain, shown in Figure 8, with blockage correction shown in Figure 9, with theory according to (Glauert, 1933) while VOF method underpredicted the drag. However, due to fluctuations of drag force in a transient model, these deviations are allowable and validates the proposed model.

Transient analysis and the cylinder in another position and with higher blockage ratios are still required for the complete validation of this model. However, since the propose of this work is to validate this model for blockage ration in order of used in (Bahaj, W.M.J., & McCann, 2007), the main goal was achieved.

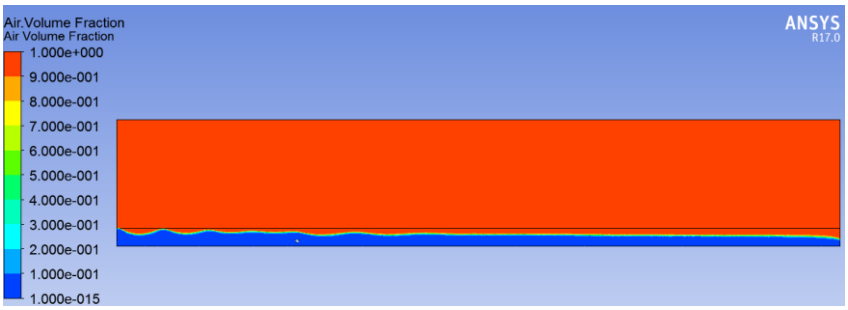

Figure 6 - Air volume fraction for biphasic flow - U = 1m/s, Re= 45000, Fr = 0,23

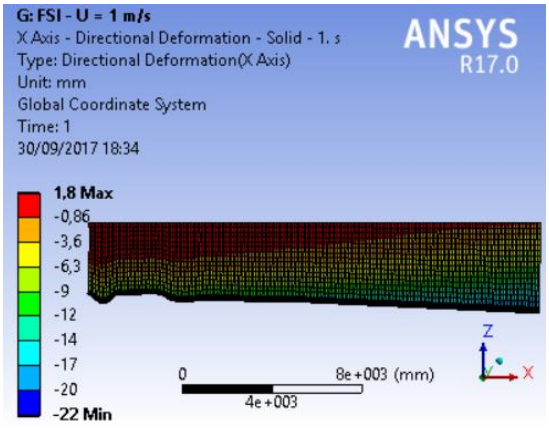

Figure 7 - Results for structure and fluid Fluid-Structure Interaction Model - U = 1m/s, Re= 45000, Fr = 0,23

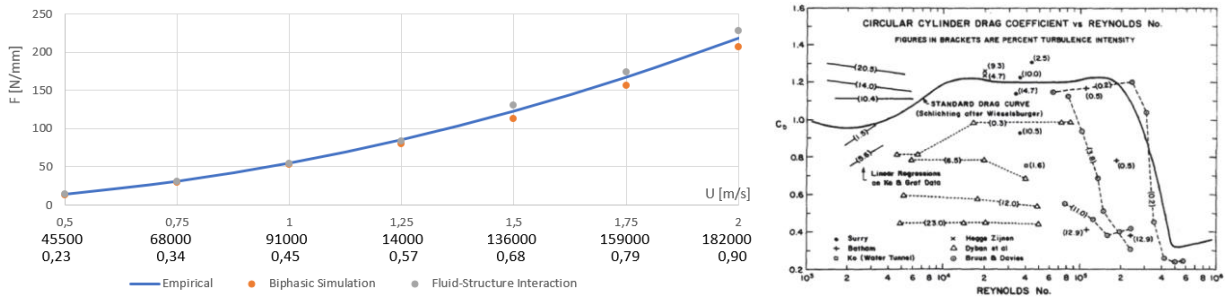

Figure 8 – Results on Left and Experimental Circular Cylinder Drag Coefficient (Bell, 1983) on Right

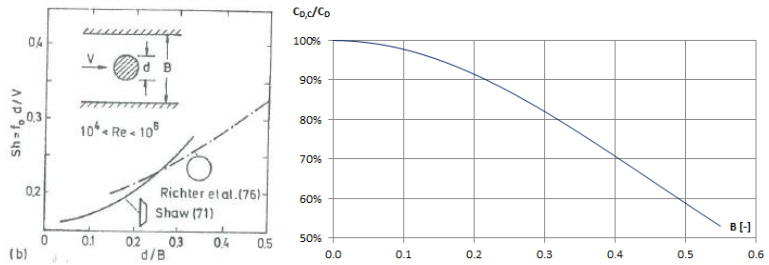

Figure 9 -Blockage Effects on vortex shedding (Naudascher & Rockwell, 1994) drag coefficient correction (Glauert, 1933)

4. CONCLUSION

The analytical approaches prove that free surface modelled by an orthotropic elastic wall gives a good approximation for biphasic flows. This is confirmed by computational simulations However, transient simulations with coupling between fluid structure are required to validate transient models.

5. REFERENCES

ANSYS Inc. (2016). *CFX 2017 Users Guide.*

ANSYS(b). (2016). *ANSYS Mechanical 17.0 Users Guide* .

Bahaj, A., W.M.J., B., & McCann, G. (2007). Experimental verifications of numerical predictions for the hydrodynamic performance of horizontal axis marine current turbines. *Renewable Energy*, 2479-2490.

Bell, W. (1983). Turbulence V.S. Drag - Some Future Consideration. *Ocean Engineering Vol. 10*, pp. 47-63.

Capaldi, F. (2012). *Continuum Mechanics - Constitutive Modeling of Structural and Biological Materials.* New York: Cambridge University Press.

Glauert, H. (1933). Wind tunnel interference on wings, bodies and airscrews. *British ARC* .

Houlsby, G., Draper, S., & Oldfield, M. (2007). *Application of Linear Momentum Actuator Disc Theory to Open Channel Flow.* Oxford: University of Oxford - Department of Engineering Science.

Ketabdari, M. (2016). Free surface flow simulation using VOF method. Em M. Ketabdari, *Numerical Simulation - From brain imaging to turbulent flows* (pp. 365-398). Intech.

Lanczos, C. (1949). *Variational principles of mechanics.* New York: Dover.

Lekhnitskii, S. (1981). *Theory of Elasticity of an Anisotropic Body.* Moscow: Mir Publishers.

Meirovitch, L. (2001). *Fundamentals of Vibrations.* New York: McGraw Hill.

Menter, F. R. (1992). *Improved Two-Equation k-w Turbulence Models for Aerodynamic Flows.* NASA. Washington D.C.: National Aeronautics and Space Administration.

Naudascher, E., & Rockwell, D. (1994). Factors affecting vortex shedding. Em E. Naudascher, & D. Rockwell, *Flow-Induced Vibrations - An Engineering Guide* (pp. 127-135). New York: Dover.

Newman(b), & J.N. (1977). Finite Depth Effects. Em Newman(b), & J.N., *Marine Hydrodynamics* (pp. 243-246). Massachucetts: MIT Press.

Newman, J. (1977). Linearized Free-Surface Condition. Em J. Newman, *Marine Hydrodynamics* (pp. 238- 240). Massachusetts: MIT Press.

Pope, A. (1951). The Velocity Potential. Em A. Pope, *Basic Wing and Airfoil Theory* (pp. 62-64). McGraw hill.

Pope, S. B. (2000). The Equations of Fluid Motion - The Role of Pressure. Em S. Pope, *Turbulent Flows* (pp. 15-19). Cambridge: Cambridge University Press.

Rao, S. (2016). *Mechanical Vibrations 6th Edition.* Pearson Education.

Timoshenko, S., & Goodier, J. (2010). *Theory of Elasticity - Third Edition.* New York: McGraw Hill.

Whelan, J., Thomson, M., Graham, J., & Peiró, J. (Januart de 2007). Modelling of free surface proximity and wave induced belocities aroung a horizontal axis tidal stream turbine. *Procedings of the 7th European Wave and Tidal Energy Conference*.

White(b), F. (2006). Conservation of Momentum: The Navier Stokes Equation. Em F. White(b), *Viscous Fluid Flow Third Edition* (pp. 62 - 64). Rhode Island: McGraw Hill.

White, F. (2006). Conditions at a Free Liquid Surface. Em F. White, *Viscous Fluid Flow Third Edition* (pp. 49-51). Rhode Island: McGraw Hill.

White, F. (2006). *Viscous Fluid Flow 3rd Ed.* New York: McGraw-Hill.

White, F. M. (1998). The linear momentum equation. Em M. White, *Fluid Mechanics 4th Edition* (pp. 146-156). Rhode Island: McGraw Hill.

World Energy Council. (2016). *World Energy Resources - Marine Energy.* London: World Energy Council.

6. RESPONSIBILITY NOTICE

The authors are the only responsible for the printed material included in this paper.